Electronic Supplementary Material (ESI) for Journal of Materials Chemistry A.

Embedding heterostructured MnS/$Co_{1-x}S$ nanoparticles in porous carbon/graphene for superior lithium storage

Baosheng Li,[a] Ruirui Wang,[a,b] Ziliang Chen,[b] Dalin Sun,[b,c] Fang Fang,[*,b,c] and Renbing Wu[*,b,c,d]

[a] Key Laboratory of Flexible Electronics & Institute of Advanced Materials (IAM), Jiangsu National Synergistic Innovation Center for Advanced Materials, Nanjing Tech University, Nanjing 211816, P. R. China.

[b] Department of Materials Science, Fudan University, Shanghai 200433, P. R. China

[c] Shanghai Innovation Institute for Materials, Shanghai 200444, P. R. China.

[d] Guangdong Provincial Key Laboratory of Advanced Energy Storage Materials, South China University of Technology, Guangzhou 510640, P. R. China

Table S1. Comparison of electrochemical performances of $MnS/Co_{1-x}S@C@rGO$ composites electrode with previously reported manganese- and cobalt-based electrodes.

Products	***Synthetic method***	***Electrode formulation***[a]	***Cycling stability(A/B/n)***[b]	***Ref.***
$MnS/Co_{1-x}S@C@rGO$	Hydrothermal and thermal annealing	70:20:10	1018/1/500	This work
MnS@C	In situ co-pyrolysis	80:10:10	200/0.5/800	[S1]
coral-like α-MnS-NC	Hydrothermal and thermal annealing	80:10:10	699/0.5/500	[S2]
MnS/RGO	Hydrothermal	70:20:10	830/0.5/100	[S3]
MnS microboxes	Solvothermal and thermal annealing	70:20:10	495/0.2/100	[S4]
MnO/C microsheets	Thermal annealing	80:10:10	798/0.1/50	[S5]
Mn_3O_4 tetragonal bipyramids	Hydrothermal	70:20:10 (CMC)[c]	822/0.2/50	[S6]
MnO/C-N	Immersion-annealing route	80:10:10	513/0.3/400	[S7]
CoS_2/NCNTF	MOF-derivation	70:20:10	937/1/160	[S8]
Co_9S_8/N-C	MOF-derivation	70:10:20 (CMC)[c]	784/0.5/400	[S9]
NC/CoS_2	MOF-derivation	70:20:10	560/0.1/50	[S10]
CNT@CoS@C	Thermal annealing	80:10:10 (CMC)[c]	1010/0.5/200	[S11]
hollow CoS_2@C	Solvothermal and the calcination	80:10:10 (PTFE)[d]	730/0.5/200	[S12]

[a]means weight ratio of the active material, carbon and binder. PVDF was used as binder if not mentioned. Other values used were specified.

[b]*A*/*B*/*n* means the capacity of *A* (mAh g^{-1}) at the certain current density of *B* (A g^{-1}).

[c]CMC means carboxymethyl cellulose. [d]PTFE means polytetrafluorethylene.

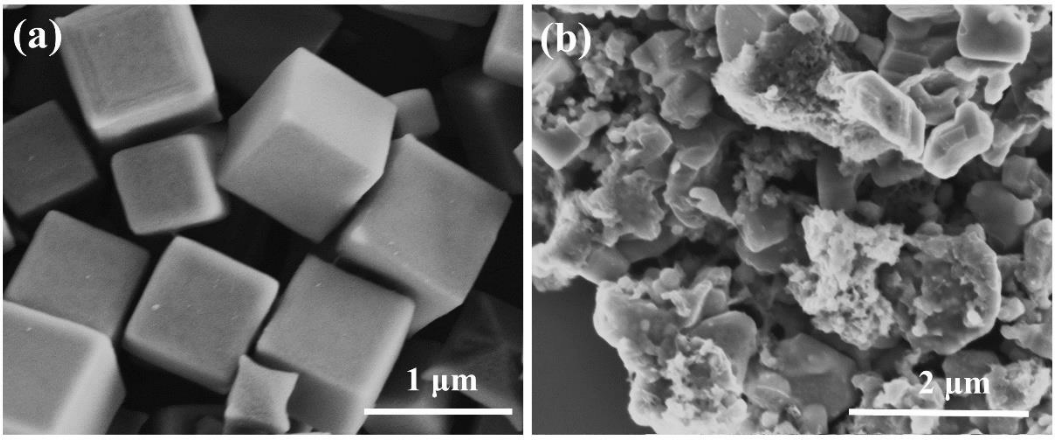

Fig. S1 FESEM images of (a) $Mn_3[Co(CN)_6]_2 \cdot 9H_2O$ precursor and (b) $MnS/Co_{1-x}S@C$.

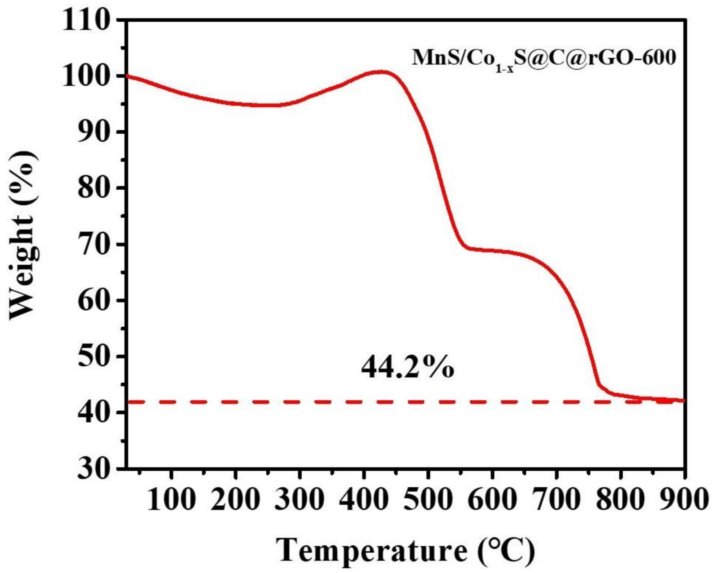

Fig. S2 TGA curve of the as-prepared $MnS/Co_{1-x}S$@C@rGO-600 composite.

The atomic ratio of Mn, Co, S elements in $MnS/Co_{1-x}S$@C@rGO-600 was determined to be about 1.5:1:2.6 by the ICP measurement.

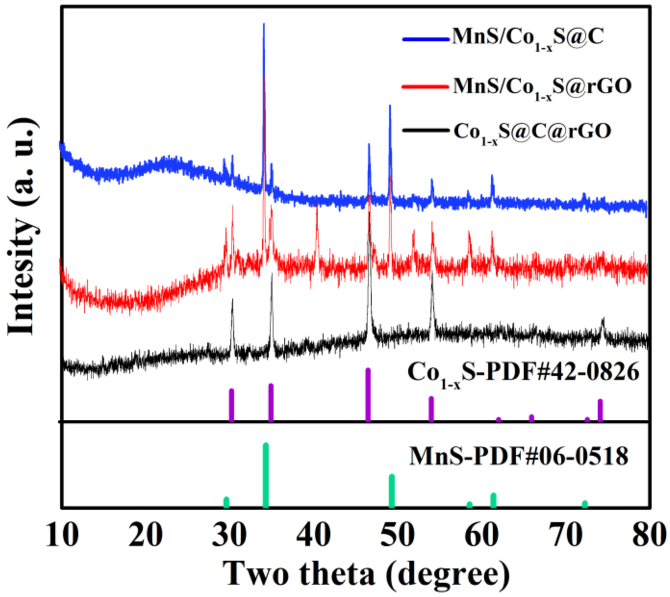

Fig. S3 XRD patterns of $MnS/Co_{1-x}S@C$, $MnS/Co_{1-x}S@rGO$ and $Co_{1-x}S@C@rGO$ composites.

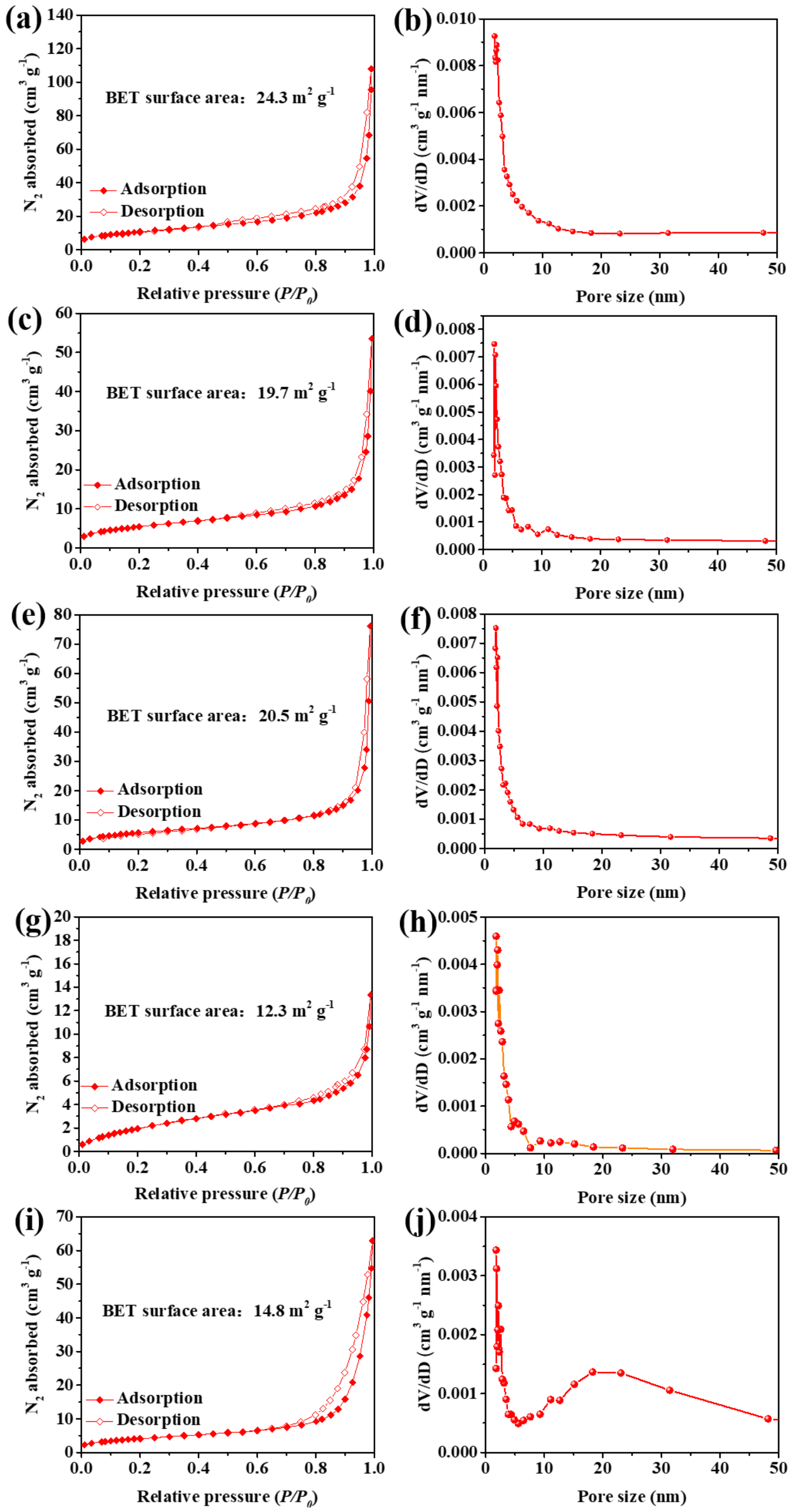

Fig. S4 N_2 sorption isotherms and the corresponding pore-size distributions based on the Barrett–Joyner–Halenda (BJH) method (a,b) MnS/Co_{1-x}S@C@rGO-500, (c,d) MnS/Co_{1-x}S@C@rGO-700, (e,f) Co_{1-x}S@C@rGO, (g,h) MnS/Co_{1-x}S@rGO and (i,j) MnS/Co_{1-x}S@C composites.

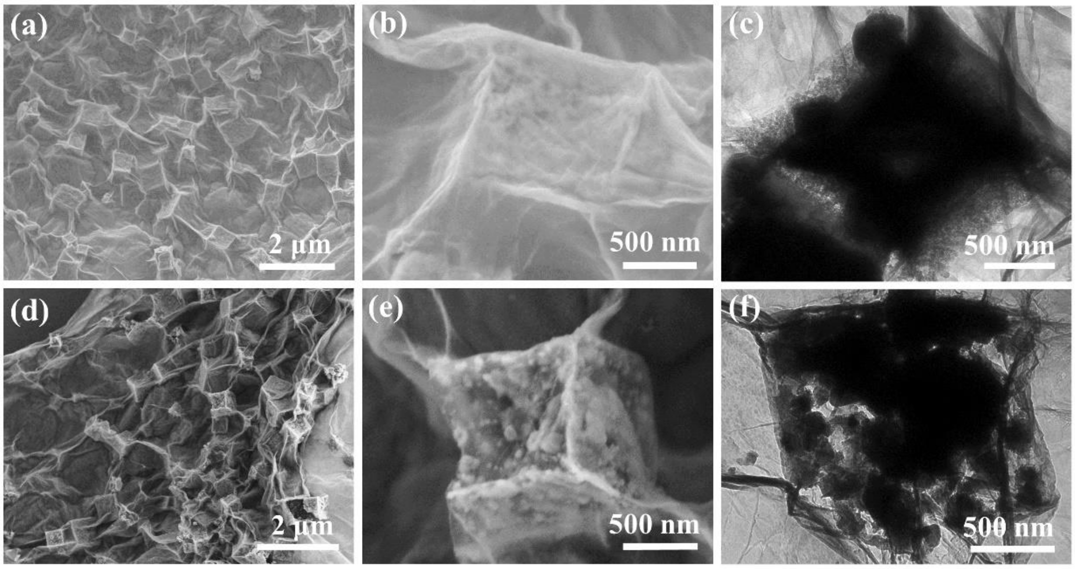

Fig. S5 (a,b) FESEM images and (c) TEM image of MnS/$Co_{1-x}S$@C@rGO-500; (d,e) FESEM images and (f) TEM image of MnS/$Co_{1-x}S$@C@rGO-700.

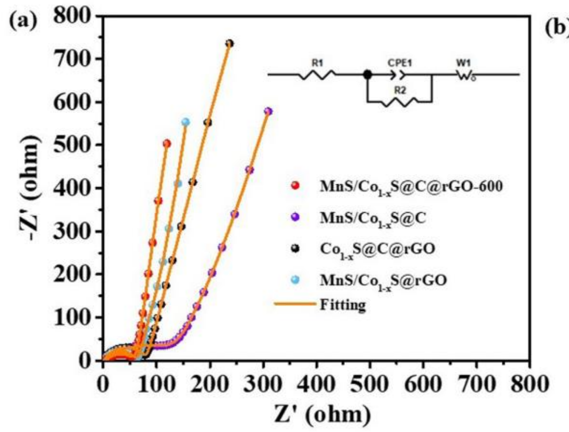

(b)

	Rs (Ω)
MnS/Co_{1-X}S@C@rGO-600	1.42
MnS/Co_{1-X}S@C	3.67
Co_{1-X}S@C@ rGO	3.14
MnS/Co_{1-X}S@ rGO	2.45

Fig. S6 (a) The EIS curves and (b) Rs values of the MnS/Co_{1-x}S@C@rGO-600, MnS/Co_{1-x}S@C, Co_{1-x}S@C@rGO and MnS/Co_{1-x}S @rGO composites electrodes.

.

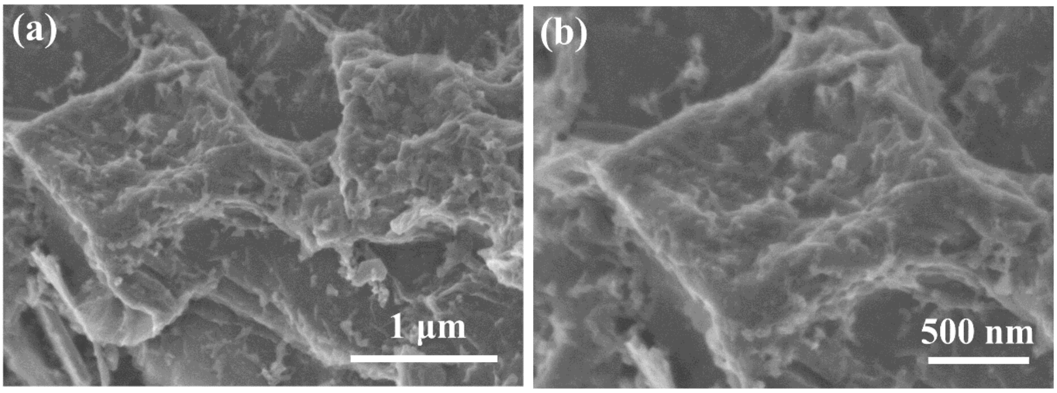

Fig. S7 (a,b) FESEM images MnS/$Co_{1-x}S$@C@rGO electrode after 500 cycles at a current density of 1 A g^{-1}.

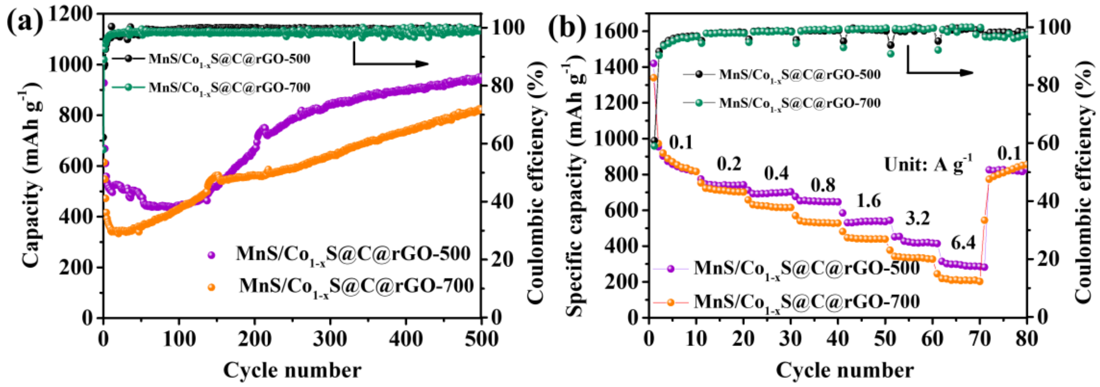

Fig. S8 (a) Cycling performance at 1 A g^{-1} and (b) rate capabilities at various current densities of MnS/Co$_{1-x}$S@C@rGO-500 and MnS/Co$_{1-x}$S@C@rGO-700 electrodes.

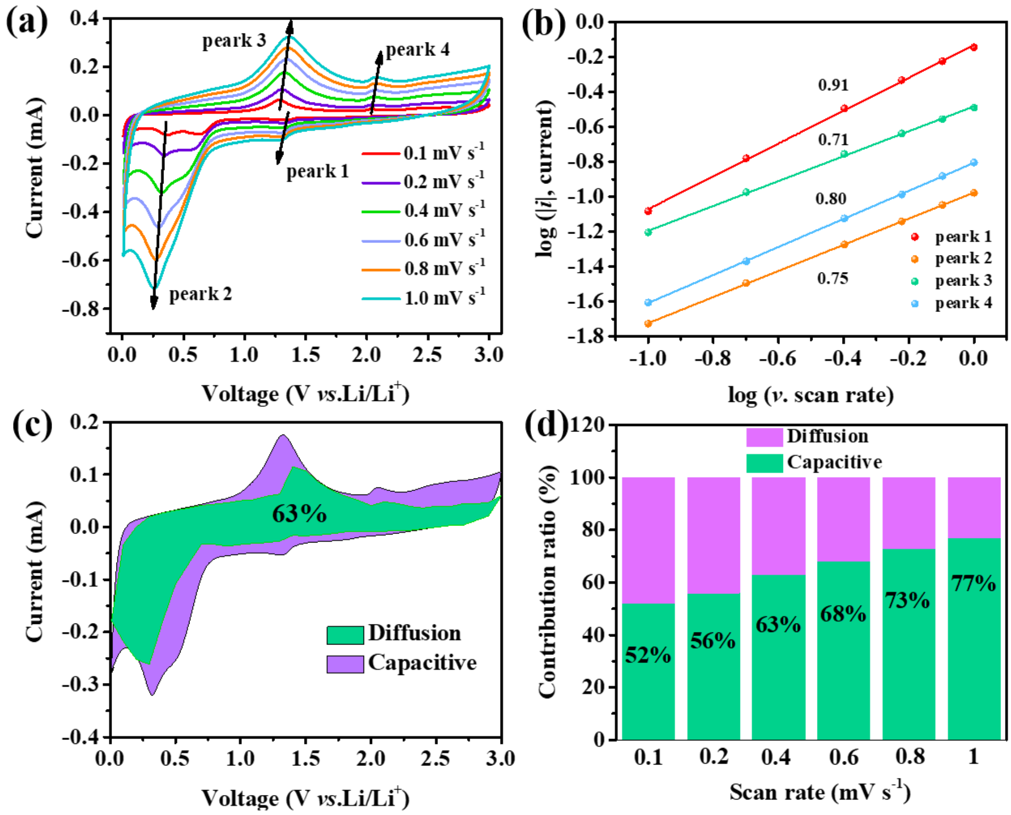

Fig. S9 (a) CV curves of $MnS/Co_{1-x}S$@rGO electrode at various sweep rates, (b) log i/log v plots at oxidized and reduced state of $MnS/Co_{1-x}S$@rGO electrode, (c) the capacitive and diffusion-controlled contribution to all charge storage of $MnS/Co_{1-x}S$@rGO electrode at the sweep rate of 0.4 mV/s, (d) the normalized contribution percentage from capacitive-controlled and diffusion-controlled behaviour for all charge storage at different sweep rates.

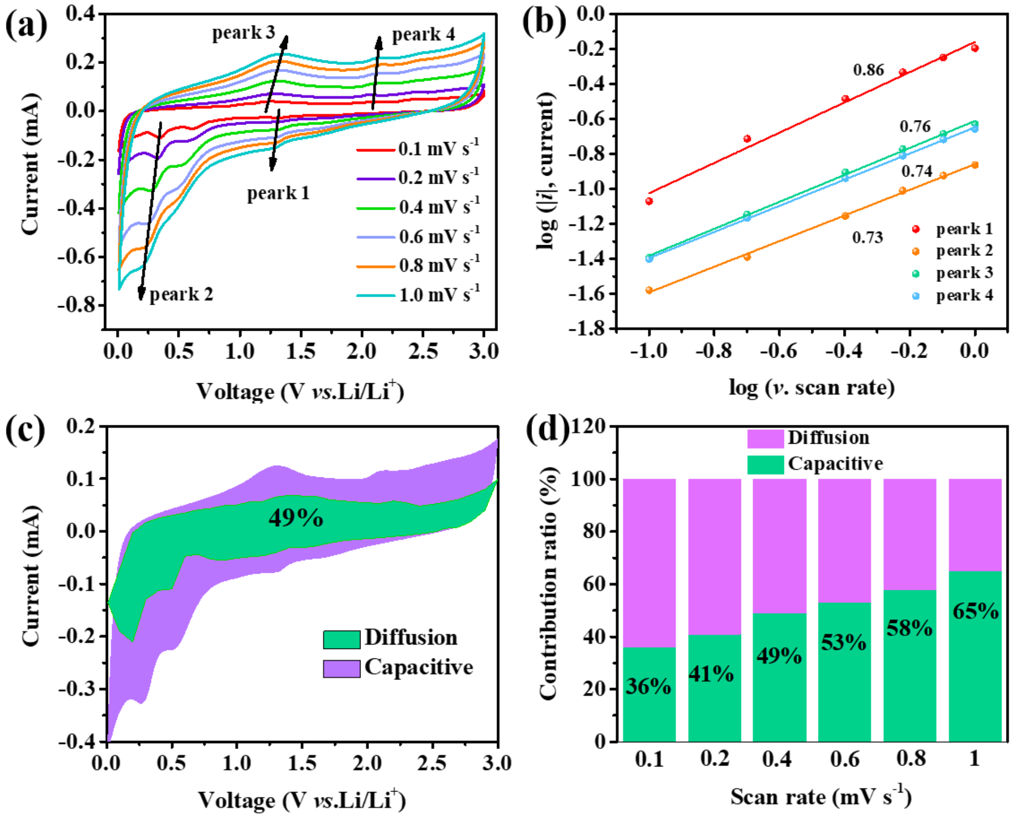

Fig. S10 (a) CV curves of $MnS/Co_{1-x}S@C$ electrode at various sweep rates, (b) log i/log v plots at oxidized and reduced state of $MnS/Co_{1-x}S@C$ electrode, (c) the capacitive and diffusion-controlled contribution to all charge storage of $MnS/Co_{1-x}S@C$ electrode at the sweep rate of 0.4 mV/s, (d) the normalized contribution percentage from capacitive-controlled and diffusion-controlled behaviour for all charge storage at different sweep rates.

References

S1 J. Y. Ning, D. Zhang, H. H. Song, X. H. Chen and J. S. Zhou, *J. Mater. Chem. A*, 2016, **4**, 12098–12105.

S2 Y. Liu, Y. Qiao, W. X. Zhang, Z. Li, X. L. Hu, L. X. Yuan and Y. H. Huang, *J. Mater. Chem.*, 2012, **22**, 24026–24033.

S3 X. J. Xu, S. M. Ji, M. Z. Gu and J. Liu, *ACS Appl. Mater. Interfaces*, 2015, **7**, 20957−20964.

S4 L. Zhang, L. Zhou, H. B. Wu, R. Xu and X. W. Lou, *Angew. Chem. Int. Ed.*, 2012, **51**, 7267–7270.

S5 J. L. Liu, N. Chen and Q. M. Pan, *J. Power Sources*, 2015, **299**, 265–272.

S6 T. T. Li, C. L. Guo, B. Sun, T. Li, Y. G. Li, L. F. Hou and Y. H. Wei, *J. Mater. Chem. A*, 2015, **3**, 7248–7254.

S7 L. F. Chen, S. X. Ma, S. Lu, Y. Feng, J. Zhang, S. Xin and S. H. Yu, *Nano Res.*, 2017, **10**, 1–11.

S8 J. T. Zhang, L. Yu and X. W. Lou, *Nano Res.*, 2017, **10**, 4298–4304.

S9 P. Y. Zeng, J, W. Li, M. Ye, K. F. Zhuo and Z. Fang, *Chem. Eur. J.*, 2017, **23**, 9517–9524.

S10 Q. F. Wang, R. Q. Zou, W. Xia, J. Ma, B. Qiu, A. Mahmood, R. Zhao, Y. Y. C. Yang and D. G. Xia, Q. Xu, *Small*, 2015, **11**, 2511–2517.

S11 F. Han, C. Z. Zhang, B. Sun, W. Tang, J. X. Yang and X. K. Li, *Carbon*, 2018, **118**, 731–742.

S12 W. W. Chen, T. T. Li, Q. Hu, C. P. Li and H. Guo, *J. Power Sources*, 2015, **286**, 159–165.